An x-ray powder diffraction study of the high temperature phase transitions in α-quartz-type $AlPO_4$–$GaPO_4$ solid solutions

2005 J. Phys.: Condens. Matter 17 4463

(http://iopscience.iop.org/0953-8984/17/28/006)

INSTITUTE OF PHYSICS PUBLISHING JOURNAL OF PHYSICS: CONDENSED MATTER

J. Phys.: Condens. Matter **17** (2005) 4463–4474 doi:10.1088/0953-8984/17/28/006

An x-ray powder diffraction study of the high temperature phase transitions in α-quartz-type $AlPO_4$–$GaPO_4$ solid solutions

J Haines[1], O Cambon[1], G Fraysse[1] and A van der Lee[2]

[1] Laboratoire de Physicochimie de la Matière Condensée, UMR CNRS 5617, Université Montpellier II, cc 003, Place E Bataillon, F-34095 Montpellier, Cedex 5, France
[2] Institut Européen des Membranes de Montpellier, UMR-CNRS 5635, Université Montpellier II, cc 047, 300 Avenue Prof. E Jeanbrau, F-34095 Montpellier, Cedex 5, France

E-mail: jhaines@lpmc.univ-montp2.fr

Received 10 May 2005, in final form 14 June 2005
Published 1 July 2005
Online at stacks.iop.org/JPhysCM/17/4463

Abstract

$Al_{1-x}Ga_xPO_4$ solid solutions ($x = 0.3$, 0.7) with the α-quartz-type structure were investigated up to 1208 K by x-ray powder diffraction. The composition $Al_{0.7}Ga_{0.3}PO_4$ exhibits almost simultaneous transitions to the β-quartz and β-cristobalite forms at close to 1050 K. The tendency towards the β-quartz type structure is found to be much less marked for the Ga-rich composition ($x = 0.7$) based on the temperature dependence of the cell parameters, molar volume, fractional atomic coordinates and tetrahedral tilt angle. Direct transformation to the β-cristobalite form begins close to 1123 K. The β-quartz form exists as a stable phase only for values below $x = 0.3$.

(Some figures in this article are in colour only in the electronic version)

1. Introduction

The properties and stability of α-quartz are of great interest in the fields of Earth and materials science, crystal chemistry and solid state physics. Extending these studies to α-quartz homeotypes (GeO_2, BeF_2, PON and ABO_4 where A = B, Al, Ga, Fe; B = P, As) [1–11] provides models for SiO_2 and new materials with potentially improved properties for various technological applications, in particular as piezoelectric resonators.

Structure–property relationships have been developed for α-quartz homeotypes, linking a number of physical, dielectric and piezoelectric properties to the structural distortion with respect to the β-quartz structure type [1–11]. The structure type adopted by the ABO_4 compounds (space group $P3_121$ or $P3_221$, $Z = 3$, as for α-quartz) corresponds to a cation-ordered derivative of the α-quartz type with a doubled **c** parameter (figure 1). The structural distortion can be described in terms of the intertetrahedral bridging angle θ and the tetrahedral

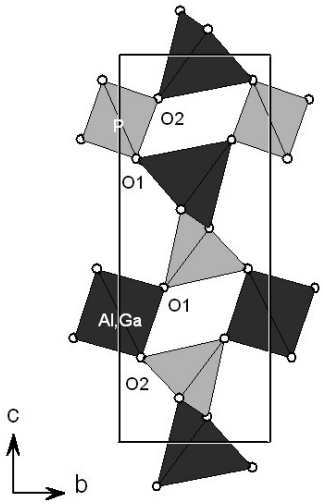

Figure 1. Polyhedral representation of the crystal structure of α-quartz-type $Al_{0.7}Ga_{0.3}PO_4$ at 298 K. Al, GaO_4 and PO_4 tetrahedra are shaded dark and light grey, respectively. The angles δ_1(Al, GaO_4), δ_2(Al, GaO_4), δ_1(PO_4) and δ_2(PO_4) (see the text) correspond to the tilt of the bond vectors Al, Ga–O1, Al, Ga–O2, P–O1 and P–O2 with respect to $\pm 45°$ (i.e. their orientation in the β-quartz-type structure).

tilt angle δ (note [12] that for α-quartz at room temperature $\theta = 143.6°$, $\delta = 16.4°$, and for β-quartz at 848 K $\theta = 153.3°$, $\delta = 0°$). The tilt angle δ can also be taken as the order parameter for the α–β phase transition in these materials [13]. In the case of ABO_4 compounds, the AO_4 and BO_4 tetrahedra have distinct tilt angles. Both the piezoelectric properties, in particular the electromechanical coupling coefficient of piezoelectric resonators, and the thermal stability improve as a function of structural distortion.

Several solid solutions exist among α-quartz homeotypes (SiO_2–GeO_2 [14, 15], SiO_2–PON [4], SiO_2–$AlPO_4$ [16], $AlPO_4$–$GaPO_4$ [17–20], $AlPO_4$–$AlAsO_4$ [17], $AlPO_4$–$FePO_4$ [21]). It was shown that, for example, in the $Al_{1-x}Ga_xPO_4$ system [20], the structural distortion (i.e. θ and δ) varies in an essentially linear way as a function of x. This may open the way to tune the piezoelectric properties of crystals in this system by varying the composition. Similarly, the thermal stability with respect to the β-quartz structure type will vary as a function of initial structural distortion by changing composition. There are however, other phase transitions, which intervene at high temperature, in particular, reconstructive transitions to tridymite or β-cristobalite forms [17, 19, 22–25]. The study of the high-temperature behaviour of the $Al_{1-x}Ga_xPO_4$ system enables the thermal stability of the α-quartz type forms and the competition between various phase transitions to be investigated by modifying the relative occupation (x) of the A cation site without changing the nature of the cation as in previously described structure–property relationships.

2. Experimental section

$Al_{1-x}Ga_xPO_4$ powder samples were prepared by hydrothermal methods as described previously [17]. Suitable quantities of solutions of $AlPO_4$ and $GaPO_4$ in sulfuric acid were mixed (with $x = 0.2$ and 0.52, respectively due to differences in solubility), placed in a PTFE-lined autoclave and heated in order to induce crystallization of $Al_{0.7}Ga_{0.3}PO_4$ and

$Al_{0.3}Ga_{0.7}PO_4$, respectively. The resulting powders were ground, passed through a 20 μm sieve and annealed at 500 °C (to eliminate the hydrated compounds eventually present in the powder).

High temperature x-ray powder diffraction measurements were performed on a PanAnalytical X'Pert diffractometer equipped with an X'Celerator detector using Ni-filtered, Cu Kα radiation. The powder samples were placed in the ceramic spinning sample holder of an Anton Paar HTK 1200 high-temperature oven-chamber. X-ray diffraction data were obtained from 19° to 124° in 2θ with a 0.008° step size over the temperature range up to 1208 K. The heating rate between points was 10 K min^{-1} with the overshoot limited to 1 K. Acquisition times were approximately 3 h. The maximum number of counts was in the order of 15 000. Rietveld refinements were performed with the program FULLPROF [26]. Due to the relatively low scattering factor of oxygen, slack constraints were applied to the Al, Ga–O and P–O distances. Generalized S_{hkl} microstrain parameters were used to account for hkl-dependent line broadening [27].

3. Results and discussion

3.1. Ambient-temperature x-ray powder diffraction

The two compositions, $Al_{0.7}Ga_{0.3}PO_4$ and $Al_{0.3}Ga_{0.7}PO_4$, were first investigated at ambient temperature by x-ray powder diffraction, tables 1 and 2. Preferential broadening of hkl reflections with $h > l$ was observed. This was interpreted in terms of microstrain linked in particular to local variations in composition [27]. Compositional gradients of up to 2% were previously detected by electron microprobe analysis of single crystals prepared in the same way [20]. The fractional coordinates of the cations compare well with previous results obtained by single-crystal diffraction [20]. The fits were relatively insensitive to the fractional coordinates of oxygen and slack constraints on the Al, Ga–O and P–O distances were needed. The c/a ratio can be considered as a very good measure of the composition x as it is relatively insensitive to zero-point and sample displacement errors. Based on a Vegard law dependence of c/a between the $AlPO_4$ and $GaPO_4$ end-members, the compositions are within 1% of the nominal target compositions. The c/a values are also consistent with the previous measurements on $Al_{1-x}Ga_xPO_4$ samples by several groups [17–20].

3.2. Stability of the α-quartz-type forms and phase transitions at high temperature

The composition $Al_{0.7}Ga_{0.3}PO_4$ was studied up to 1133 K (figures 2–4). The structure could be refined using an α-quartz-type structural model (figure 2, tables 1 and 2) up to 1023 K. A much more complex line shape was observed in the diffraction data obtained at 1073 and 1103 K (figure 3). The data for each quartz-type reflection were composed of two closely spaced Kα_1–Kα_2 doublets indicating the presence of two quartz forms, one of which was the α-quartz-type phase. The reflections corresponding to the second phase were shifted to lower 2θ values, indicating that the unit cell volume is larger. The relative proportion of this second phase increased as a function of temperature, and at 1133 K refinement was performed using a β-quartz structural model (figure 4, tables 1 and 2). The diffraction lines of the β-quartz-type phase were sharp and hkl-dependent line broadening could not be detected. In contrast, line broadening was still present in the remaining α-quartz-type phase at 1073 and 1103 K. It can be expected that the same compositional gradient persists in the β-quartz form, but in this disordered structure with a larger cell volume its effect on the line widths appears to be less marked.

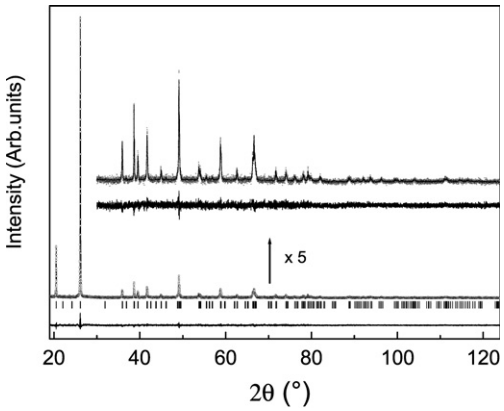

Figure 2. Experimental data (+), calculated and difference profiles (solid lines) from the Rietveld refinements of α-quartz-type $Al_{0.7}Ga_{0.3}PO_4$ at 973 K using x-ray diffraction data. Intensity is in arbitrary units and the difference profile is on the same scale. Vertical bars indicate the positions of all calculated reflections.

Table 1. Unit cell parameters, molar volume and agreement factors for quartz-type $Al_{1-x}Ga_xPO_4$ as a function of temperature. Only data for the principal phase (α-quartz) are given at 1073 and 1103 K.

T (K)	a (Å)	c (Å)	V (cm^3 mol^{-1})	R_p (%)	R_{wp} (%)	R_B (%)	χ^2
			$x = 0.3$				
298	4.9295(1)	10.9743(2)	46.356(1)	26.2	18.3	7.5	1.7
473	4.9436(1)	10.9896(2)	46.689(1)	30.9	19.0	7.9	0.8
673	4.9638(1)	11.0105(2)	47.162(1)	32.1	19.0	6.9	0.8
873	4.9868(1)	11.0341(2)	47.704(2)	34.2	19.6	8.5	0.8
973	5.0006(2)	11.0476(3)	48.026(2)	34.4	19.5	6.6	0.8
1023	5.0090(2)	11.0567(3)	48.226(2)	38.3	21.9	6.1	1.0
1073	5.0208(2)	11.0693(3)	48.508(2)	39.1	21.5	8.4	1.0
1103	5.0293(2)	11.0787(3)	48.714(3)	39.2	21.4	10.8	0.9
1133[a]	5.0472(1)	11.0890(3)	49.107(2)	43.0	23.4	6.4	1.1
			$x = 0.7$				
303	4.9143(1)	11.0139(2)	46.239(1)	29.7	18.0	9.4	0.9
473	4.9278(1)	11.0256(2)	46.542(1)	32.0	19.2	11.2	1.1
673	4.9460(1)	11.0417(2)	46.954(1)	29.7	17.2	8.6	0.8
873	4.9653(1)	11.0596(2)	47.400(1)	30.4	16.7	9.1	0.9
1023	4.9811(1)	11.0730(2)	47.759(2)	31.2	16.9	9.9	0.9
1123	4.9940(1)	11.0838(2)	48.054(2)	33.0	18.0	10.0	1.0
1173	5.0014(1)	11.0891(2)	48.218(2)	33.2	18.1	9.6	1.0
1208	5.0075(1)	11.0933(2)	48.356(2)	34.1	18.5	10.1	1.1

[a] β-quartz form.

The coexistence of the α- and β-quartz forms is unusual for α-quartz homeotypes. Although the transition is displacive and first order, there have been no previous reports of phase coexistence in the pure compounds. However, the observed coexistence of phases in the present study would appear to be consistent with a variation in transition temperature as a function of composition and the existence of long-range (μm) and short-range (nm)

Table 2. Fractional atomic coordinates and isotropic atomic displacement parameters (Å^2) for quartz-type $Al_{1-x}Ga_xPO_4$. α: $P3_121$–(Al, Ga) on 3*a* (x, 0, 1/3), P on 3*b* (x, 0, 5/6), O1, O2 on 6*c* (x, y, z). β: $P6_422$–(Al, Ga) on 3*d* (x, 0, 1/2), P on 3*c* (x, 0, 0), O1, O2 on 12*k* (x, y, z).

T (K)	$x_{(Al,Ga)}$	B_{iso}	x_P	B_{iso}	x_{O1}	y_{O1}	z_{O1}	B_{iso}	x_{O2}	y_{O2}	z_{O2}	B_{iso}
						$x = 0.3$						
298	0.4588(1)	2.44(5)	0.4572(1)	3.20(7)	0.413(1)	0.299(1)	0.3988(4)	5.4(1)	0.402(1)	0.254(1)	0.8858(4)	5.4(1)
473	0.4624(7)	1.83(6)	0.4570(5)	3.07(9)	0.430(2)	0.301(1)	0.3987(5)	4.8(1)	0.406(2)	0.254(1)	0.8884(6)	4.8(1)
673	0.4656(7)	2.26(6)	0.4640(7)	3.61(9)	0.430(2)	0.294(1)	0.4001(5)	5.6(1)	0.407(2)	0.246(1)	0.8905(6)	5.6(1)
873	0.4713(8)	2.68(7)	0.4677(7)	4.2(1)	0.424(2)	0.283(1)	0.4039(6)	7.0(2)	0.410(2)	0.241(1)	0.8934(7)	7.0(2)
973	0.4749(9)	3.00(8)	0.4698(7)	4.4(1)	0.423(2)	0.271(2)	0.4087(8)	8.4(2)	0.410(2)	0.235(2)	0.8961(8)	8.4(2)
1023	0.477(1)	2.84(8)	0.4694(7)	4.6(1)	0.426(3)	0.266(2)	0.411(1)	9.2(2)	0.411(3)	0.227(2)	0.903(1)	9.2(2)
1133[a]	0.5000	5.2(1)	0.5000	6.0(1)	0.421(1)	0.226(2)	0.587(1)	9.8(1)				
1133[b]	*0.5000*	*5.2(1)*	*0.5000*	*6.0(1)*	*0.421(1)*	*0.226(2)*	*0.420(1)*	*9.8(1)*	*0.421(1)*	*0.193(2)*	*0.913(1)*	*9.8(1)*
						$x = 0.7$						
303	0.4584(1)	2.04(4)	0.4577(1)	2.29(6)	0.401(1)	0.302(1)	0.3979(3)	3.7(1)	0.417(1)	0.273(1)	0.8747(2)	3.7(1)
473	0.4567(4)	2.11(4)	0.4607(5)	2.80(7)	0.409(1)	0.295(1)	0.3993(4)	3.8(1)	0.418(1)	0.270(1)	0.8774(3)	3.8(1)
673	0.4604(5)	2.41(4)	0.4612(5)	3.16(7)	0.411(2)	0.292(1)	0.3999(4)	5.3(1)	0.415(1)	0.265(1)	0.8812(5)	5.3(1)
873	0.4626(5)	2.74(4)	0.4671(6)	3.73(7)	0.410(2)	0.284(1)	0.4004(4)	6.1(1)	0.418(2)	0.261(1)	0.8839(5)	6.1(1)
1023	0.4653(5)	3.07(4)	0.469(1)	4.33(8)	0.413(2)	0.281(1)	0.4016(5)	6.6(2)	0.416(2)	0.257(1)	0.8859(5)	6.6(2)
1123	0.4671(6)	3.25(5)	0.469(1)	4.61(8)	0.417(3)	0.279(2)	0.4036(6)	7.6(2)	0.415(3)	0.251(1)	0.8904(6)	7.6(2)
1173	0.4695(6)	3.44(5)	0.474(1)	5.09(9)	0.411(3)	0.273(1)	0.4053(6)	8.0(2)	0.421(3)	0.250(1)	0.8914(6)	8.0(2)
1208	0.4687(7)	3.63(5)	0.475(1)	5.10(9)	0.411(3)	0.270(1)	0.4059(7)	8.0(2)	0.424(3)	0.249(1)	0.8927(6)	8.0(2)

[a] β-quartz form.

[b] Italics indicate equivalent coordinates using the trigonal $P3_121$ cell with the standard origin (i.e. shifted by 1/6 along **c** with respect to that in $P6_422$) for the β phase. O2 coordinates correspond to the atom at the equivalent position obtained by the transformation x, $x - y$, $2/3 - z$ in the hexagonal cell.

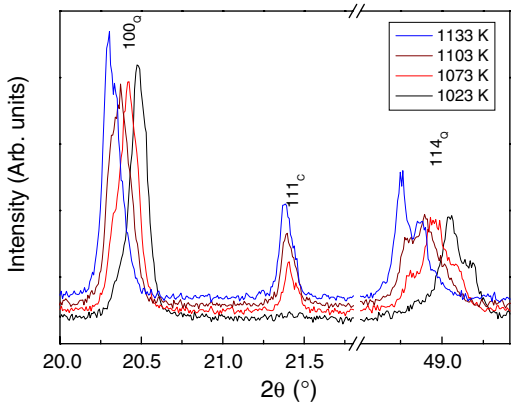

Figure 3. Selected regions in the x-ray diffraction pattern of $Al_{0.7}Ga_{0.3}PO_4$.

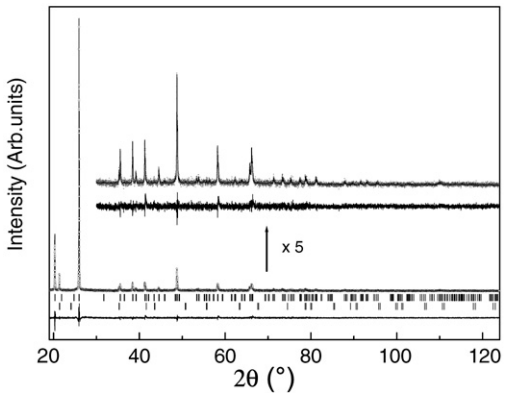

Figure 4. Experimental data (+), calculated and difference profiles (solid lines) from the Rietveld refinements of $Al_{0.7}Ga_{0.3}PO_4$ at 1133 K using x-ray diffraction data. Intensity is in arbitrary units and the difference profile is on the same scale. Vertical bars indicate the positions of all calculated reflections for the β-quartz-type (top) and β-cristobalite-type forms (bottom).

compositional gradients. Thus, in the interval over which phase coexistence is observed, the α- and β-phases correspond to two slightly different average compositions (which should vary with temperature in the coexistence region) due to the initial gradient in the sample, estimated at about 2% based on previous electron microprobe measurements [20]. The remaining α-quartz form progressively transforms to give a β-quartz-type phase with a compositional gradient similar to that existing in the initial sample. Studies of the α–β phase transition boundary by differential thermal analysis (DTA) indicate that the x–T slope is steep [17, 19].

In parallel, beginning between 1023 and 1073 K, the strongest diffraction line of the β-cristobalite form was found to appear. The quantity of this phase increased from 2.3% at 1073 K to 4.8% at 1123 K. The kinetics of this phase transition are very slow at these temperatures. The experiments to determine the phase transition temperatures on the pure end members were carried out over a period of several days [23–25]. DTA experiments are not well adapted to study these reconstructive phase transitions and typically yield temperatures significantly greater than the thermodynamic transition temperature [19].

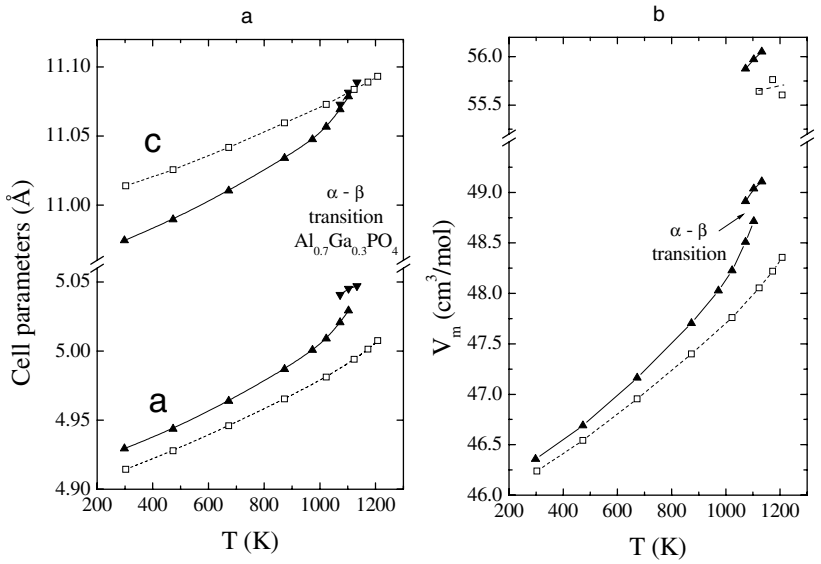

Figure 5. (a) Cell parameters of $Al_{0.7}Ga_{0.3}PO_4$ (▲, ▼) and $Al_{0.3}Ga_{0.7}PO_4$ (□) as a function of temperature. (b) Molar volume of $Al_{0.7}Ga_{0.3}PO_4$ (▲) and $Al_{0.3}Ga_{0.7}PO_4$ (□) as a function of temperature. Solid and dashed lines are guides for the eye.

The recovered sample at ambient temperature after cooling contained the α-quartz-type phase with broadened lines along with approximately 2% of the α-cristobalite form, which was obtained from cooling the high temperature β-cristobalite phase. The cell parameters of the recovered α-quartz-type form were essentially identical to those of the starting material. All the diffraction lines were slightly broader with low-angle tails, indicating some degree of volume strain eventually due to the presence of regions of intergrowth with the significantly less dense α-cristobalite form. This broadening is distinct from that which may be expected due to the presence of a compositional gradient (note for example that the a and c cell parameters vary inversely with composition). The molar volume of the α-cristobalite-type form was 51.90 cm^3 mol^{-1}, which would correspond to $x = 0.29$, based on interpolation of the data for the α-cristobalite solid solution [22].

The α-quartz phase of $Al_{0.3}Ga_{0.7}PO_4$ is much more stable as a function of temperature. The tendency towards the β-quartz type structure as found for $Al_{0.7}Ga_{0.3}PO_4$ is much less marked for this Ga-rich composition as can be seen in the temperature dependence of the cell parameters, molar volume and cation fractional x-coordinates (tables 1 and 2, figures 5 and 6). In particular, the increase in the fractional x-coordinate of Al and Ga is significantly greater for $x = 0.3$.

The tetrahedral tilt angle, δ, can be taken as an order parameter for the first-order α–β transition in quartz homeotypes. It can be noted that there are two distinct δ angles for each tetrahedron which are obtained as follows from the fractional atomic coordinates and the cell parameters:

$$\tan(45^\circ - \delta_{1(AO_4)}) = (z_{O1} - 1/3)c/y_{O1}a \sin\gamma \quad (1)$$

$$\tan(45^\circ - \delta_{2(AO_4)}) = (x_{O2-}y_{O2})a \sin\gamma/(1 - z_{O2})c \quad (2)$$

$$\tan(45^\circ - \delta_{1(PO_4)}) = (x_{O1-}y_{O1})a \sin\gamma/(1/2 - z_{O1})c \quad (3)$$

$$\tan(45^\circ - \delta_{2(PO_4)}) = (z_{O2} - 5/6)c/y_{O2}a \sin\gamma. \quad (4)$$

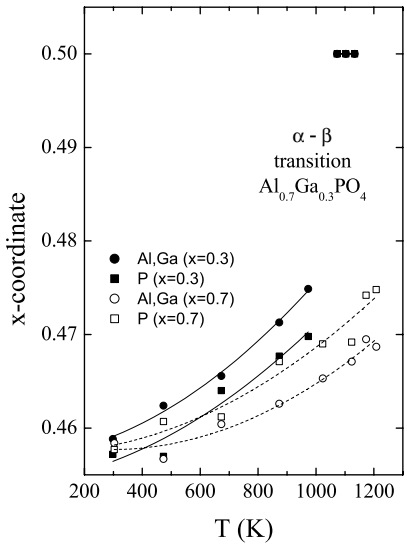

Figure 6. Cation fractional atomic coordinates of quartz-type $Al_{0.7}Ga_{0.3}PO_4$ and $Al_{0.3}Ga_{0.7}PO_4$ as a function of temperature. Solid and dashed lines are guides for the eye.

In the present case, the average value is used. It can be shown based on a Landau model that the temperature dependence of δ can be expressed as follows [13]:

$$\delta^2 = \frac{2}{3}\delta_0^2\left(1+\sqrt{1-\frac{3}{4}\frac{T-T_c}{T_{tr}-T_c}}\right) \tag{5}$$

where δ_0 is the drop in tilt angle at the transition temperature (T_{tr}) and T_c would be the temperature for a second-order transition. Whereas it can be seen that this type of behaviour occurs for $x = 0.3$, figure 7, it is not possible to accurately solve for T_c due to the relative uncertainty in T_{tr} and δ_0 resulting from gradients in composition.

Based on the above results, a transition to a β form for $x = 0.7$, if such a transition exists, would occur at temperatures well above the maximum temperature reached, 1233 K. Instead, the kinetically hindered, reconstructive transition from the α-quartz-type to the β-cristobalite form was observed beginning at 1123 K, figure 8. The β-cristobalite form was found to represent 2.7% of the total material at 1233 K. The recovered sample contained 5.6% of the α-cristobalite form with a molar volume of 50.97 cm^3 mol^{-1}. This would correspond to $x = 0.67$ [22]. The cell parameters of the α-quartz form were identical to those of the starting material.

3.3. Thermal expansion and volume changes

The thermal expansion coefficient of the α-quartz forms for $x = 0.3$ and 0.7 can be expressed as follows:

$x = 0.3$ $\quad T \geqslant 298$ K

$$\alpha_T(K^{-1}) = 4.03(11)\times 10^{-5} + 9.2(6)\times 10^{-11}(T-298)^2 \tag{6}$$

$x = 0.7$ $\quad T \geqslant 303$ K

$$\alpha_T(K^{-1}) = 3.94(6)\times 10^{-5} + 4.0(3)\times 10^{-11}(T-303)^2. \tag{7}$$

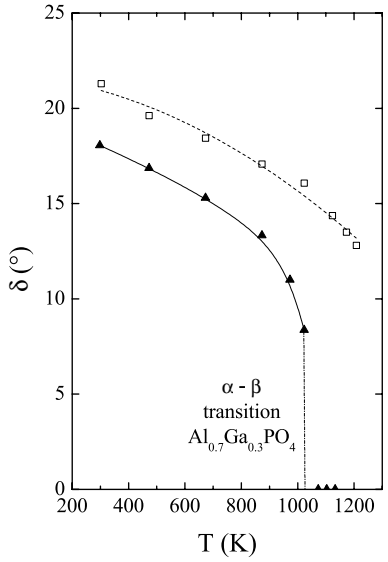

Figure 7. Evolution of the average tilt angle δ as a function of temperature for $Al_{0.7}Ga_{0.3}PO_4$ (▲) and $Al_{0.3}Ga_{0.7}PO_4$ (□). Solid and dashed lines are guides for the eye.

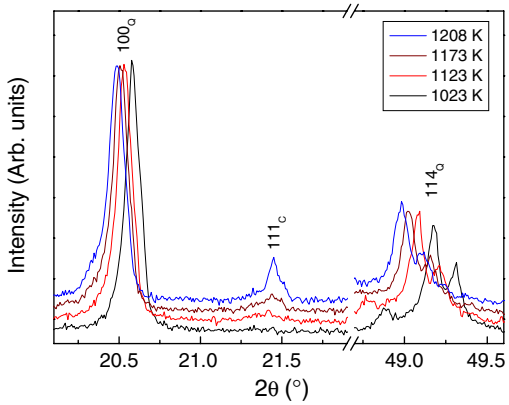

Figure 8. Selected regions in the x-ray diffraction pattern of $Al_{0.3}Ga_{0.7}PO_4$.

These thermal expansion coefficients are essentially identical to that of $AlPO_4$ (3.97×10^{-5} K^{-1}) [28] and somewhat greater than the corresponding value for $GaPO_4$ (3.0×10^{-5} K^{-1}) [29]. The second non-linear term in the expression is much greater for $x = 0.3$ due to the much higher thermal expansion prior to the α–β transition. There appears to be lower thermal expansion in the β phase based on the limited data for this phase. This is consistent with the absence of tetrahedral tilting as a potential expansion mechanism.

In spite of considerable thermal expansion, the Al, Ga–O and P–O bond lengths exhibit a strong tendency to decrease. Quite loose slack constraints were applied in the α-quartz-type phase in order to avoid unrealistic dispersion in the pairs of crystallographically distinct distances. Such constraints were unnecessary for the β-quartz-type form. The average Al, Ga–O and P–O bond lengths decreased from 1.753(5) and 1.524(5) Å, respectively at 298 K to 1.684(8) and 1.520(8) Å at 1133 K. This apparent decrease in bond length is observed

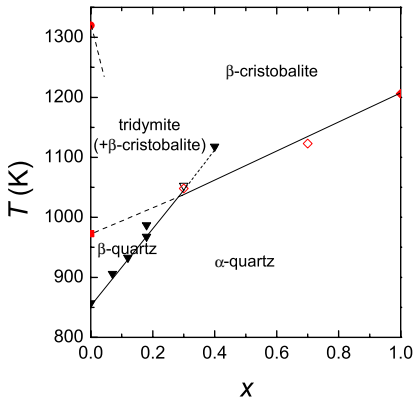

Figure 9. x–T phase diagram of $Al_{1-x}Ga_xPO_4$. Open symbols are from the present study. Solid symbols are from [17, 19, 23, 24].

for many quartz homeotypes [5, 6, 12, 28–30] and can be taken as evidence for dynamic disorder [30]. Total neutron scattering on α-quartz indicates that the actual bond distance does in fact increase, whereas the value obtained by diffraction corresponding to the time-averaged structure decreases [30].

The first order α–β quartz-type transition is associated with a small volume change of 0.8% at 1073 K for $x = 0.3$. The volume change at the same temperature for the α-quartz–β-cristobalite transition is 15.2%. This is very similar to the corresponding value for $x = 0.7$ of 15.8% at 1123 K. The ΔV values for the end-members $AlPO_4$ and $GaPO_4$ are in the range of 15–16% [22, 28, 31].

3.4. x–T phase diagram

The x–T phase diagram of $Al_{1-x}Gax PO_4$ has been previously investigated by DTA and x-ray diffraction [17, 19]. The phase boundary for the displacive α–β quartz-type transition has been determined and is in good agreement with the result obtained for $x = 0.3$ in the present study (figure 9). The temperature for the reconstructive transition to the β-cristobalite form is more difficult to determine. The transition temperature for pure $GaPO_4$ of 1206 K was obtained by high-temperature treatments lasting up to 4 days to detect the onset of the transition [24]. Similarly for $AlPO_4$, for which an intermediate tridymite type phase is present between the β quartz and β-cristobalite forms, experiments lasting several days were performed to determine the transition temperatures [23]. Tridymite was first formed beginning at 971 K and above 1320 K only β-cristobalite is formed. These structures are closely related, being based on hexagonal and cubic close packing, respectively. Mixtures of the two forms are often obtained between the two transition temperatures above [23, 25]. In the present study with a very low detection limit (<1%), it is found that experimental values are consistent with the above results for the pure end members. Due to kinetic effects, previous results by DTA place the reconstructive transition to the β-cristobalite form at higher temperatures [17, 19].

The results for the Al-rich sample indicate that the α–β quartz–β-cristobalite triple point lies slightly below $x = 0.3$ and $T = 1050$ K. The β-quartz form exists thus as a stable phase only at values of below $x = 0.3$. The metastable α–β quartz-type boundary was followed experimentally up to $x = 0.4$. Extrapolation would give a virtual transition temperature of 1310 K for $x = 0.7$, which is in agreement with the temperature dependence of δ (figure 7)

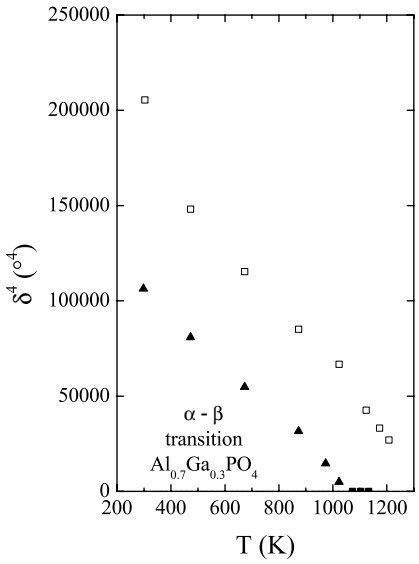

Figure 10. Evolution of δ^4 as a function of temperature for $Al_{0.7}Ga_{0.3}PO_4$ (▲) and $Al_{0.3}Ga_{0.7}PO_4$ (□).

and the tendency if one plots δ^4 [6, 13, 30] (see equation (5)) as a function of temperature (figure 10), both of which indicate that a hypothetical α–β transition would only occur above 1300 K. Further extrapolation would give 1505 K for pure $GaPO_4$, which is well above the temperature at which the transformation to the β-cristobalite form is complete. This is lower than the 1929 K predicted from a pseudo-spin Ising model based on the barrier related to tetrahedral tilting [32].

4. Conclusions

$Al_{1-x}Ga_xPO_4$ solid solutions were studied as a function of temperature by x-ray powder diffraction. The behaviour of the cell parameters, volume and atomic positions indicates that the high temperature stability of the α-quartz form increases as a function of x. This is particularly notable in the temperature dependence of the tetrahedral tilt angle δ. The sensitivity of the present method enabled the transition to the β-cristobalite form to be detected near the onset temperature. The β-quartz form is found only to exist as a stable phase for $x < 0.3$. The results have permitted an updated composition–temperature phase diagram to be proposed. This phase diagram presents the thermal behaviour covering the range of structural distortion from $\delta = 17.6°$, $\theta = 142.5°$ ($AlPO_4$) [28] to $\delta = 23.4°$, $\theta = 134.6°$ ($GaPO_4$) [29] in a continuous manner.

References

[1] Philippot E, Goiffon A, Ibanez A and Pintard M 1994 *J. Solid State Chem.* **110** 356
[2] Philippot E, Palmier D, Pintard M and Goiffon A 1996 *J. Solid State Chem.* **123** 1
[3] Philippot E, Armand P, Yot P, Cambon O, Goiffon A, McIntyre G J and Bordet P 1999 *J. Solid State Chem.* **146** 114
[4] Haines J, Chateau C, Léger J M and Marchand R 2001 *Ann. Chim. Sci. Mater.* **26** 209
[5] Haines J, Cambon O, Philippot E, Chapon L and Hull S 2002 *J. Solid State Chem.* **166** 434

[6] Haines J, Cambon O and Hull S 2003 *Z. Kristallogr.* **218** 193
[7] Cambon O, Yot P, Ruhl S, Haines J and Philippot E 2003 *Solid State Sci.* **5** 469
[8] Cambon O and Haines J 2003 *Proc. 2003 IEEE Int. Freq. Control Symp.-17th Eur. Freq. Time Forum* (Piscataway, NJ: IEEE) p 650
[9] Haines J, Cambon O, Astier R, Fertey P and Chateau C 2004 *Z. Kristallogr.* **219** 32
[10] Haines J and Cambon O 2004 *Z. Kristallogr.* **219** 314
[11] Cambon O, Haines J, Fraysse G, Détaint J, Capelle B and Van der Lee A 2005 *J. Appl. Phys.* **97** 074110
[12] Kihara K 1990 *Eur. J. Mineral.* **2** 63
[13] Grimm H and Dorner B 1975 *J. Phys. Chem. Solids* **36** 407
[14] Miller W S, Dachille F, Shafer E C and Roy R 1963 *Am. Mineral.* **48** 1024
[15] Fursenko B A, Kirkinsky V A and Rjaposov A P 1980 High-pressure science and technology *Proc. VIIth AIRAPT Int. Conf.* ed B Vodar and P Marteau (Oxford: Pergamon) p 562
[16] Veksler I V, Thomas R and Wirth R 2003 *Am. Mineral.* **88** 1724
[17] Cachau-Herreillat D, Bennazha J, Goiffon A, Ibanez A and Philippot E 1992 *Eur. J. Solid State Inorg. Chem.* **29** 1295
[18] Xia H R, Qin Z K, Yuan W, Liu S F, Zou Z Q and Han J R 1997 *Cryst. Res. Technol.* **32** 783
[19] Barz R U, David F, Schneider J and Gille P 2001 *Z. Kristallogr.* **216** 501
[20] Haines J, Cambon O, Cachau-Herreillat D, Fraysse G and Mallassagne F E 2004 *Solid State Sci.* **6** 995
[21] Mohamed F Sh 2002 *Adsorption Sci. Technol.* **20** 741
[22] Achary S N, Jayakumar O D, Tyagi A K and Kulshresththa S K 2003 *J. Solid. State Chem.* **176** 37
[23] Shafer E C and Roy R 1957 *Z. Phys. Chem.* **11** 30
[24] Shafer E C and Roy R 1956 *J. Am. Ceram. Soc.* **39** 330
[25] Flörke O W 1967 *Z. Kristallogr.* **125** 134
[26] Rodríguez-Carvajal J, unpublished
[27] Stephens P W 1999 *J. Appl. Crystallogr.* **32** 281
[28] Maruoka Y and Kihara K 1997 *Phys. Chem. Minerals* **24** 243
[29] Nakae H, Kihara K, Okuno M and Hirano S 1995 *Z. Kristallogr.* **210** 746
[30] Tucker M G, Keen D A and Dove M T 2001 *Mineral. Mag.* **65** 489
[31] Haines J, Cambon O, Prudhomme N, Fraysse G, Keen D A, Chapon L C and Tucker M G, unpublished
[32] Engel G F and Krempl P W 1984 *Ferroelectrics* **54** 9